LAND COVERS ANALYSES DURING SLASH AND BURN AGRICULTURE BY USING MULTISPECTRAL IMAGERY OBTAINED WITH UNATTENDED AERIAL VEHICLES (UAVs) †

[ANÁLISIS DE LA COBERTURA VEGETAL DURANTE LA AGRICULTURA DE TUMBA-QUEMA UTILIZANDO IMÁGENES MULTISPECTRALES OBTENIDAS CON VEHÍCULOS AÉREOS NO TRIPULADOS (VANTs)]

**Dámaso R. Ponvert-Delisles Batista, Héctor Estrada-Medina*,
Gonzalo N. Gijón-Yescas and Oscar O. Álvarez-Rivera**

*Departamento de Manejo y Conservación de Recursos Naturales Tropicales,
Facultad de Medicina Veterinaria y Zootecnia, Campus de Ciencias Biológicas y
Agropecuarias, Universidad Autónoma de Yucatán. Km. 15.5 carretera Mérida-
Xmatkuil s/n, C.P. 97315, Mérida, Yucatán, México. Email:
damaso.ponvert@gmail.com, hector.estrada@correo.uady.mx,
nefthally@gmail.com, oscaralvarez.uady@gmail.com
Corresponding author

SUMMARY

Background. The Milpa is one of the traditional agricultural systems of Yucatan, Mexico; it is implemented by using the agricultural procedure called "Slash & Burn". Quality and quantity of forest fuel (*i.e.* biomass) are two of the main factors related to burn severity. Burning affects soil properties related to fertility and crop production. The use of new approaches of remote sensing technologies such as Unattended Aerial Vehicles (UAVs), can allow studying the importance of fire in agriculture to improve productivity in slash & burn agricultural systems. **Objective**. Analyze the land covers and its influence on the severity of the agricultural burning in a "Milpa" agroecosystem with multi-spectral images acquired by UAVs. **Methodology**. The study site was located in the municipality of Tzucacab, Yucatan, Mexico. Two plots were selected [10-15 and 20-25 years of fallow]; land cover was characterized before and after slash & burn. Three multispectral sensors [Red, Green, Blue (RGB); Near Infrared (NIR) and; Thermal Infra-Red (TIR)] were mounted on UAVs, to obtained multispectral imagery and generate orthomosaics for later analyses. **Results**. With the imagery, the Normalized Difference Vegetation Index [NDVI] was calculated and its spectral behavior evaluated. The imagery was used to analyze the fire intensity. On RGB imagery, patterns of areas with greater dry biomass cover associated to high burn severity and, areas with green vegetation or naked soil associated to low burn severity were observed. Land covers with high fuel potential showed low NDVI index values. **Implications.** The analyses of the multispectral imagery taken by drones allow the quick evaluation of the land covers and the intensity of agricultural fires, with the pertinent adjustments, in the near future this could become a standard methodology to accomplish this kind of evaluations. **Conclusions**. This approach allowed to analyze the state of land covers to visually assess the quality of fuel and its influence on the intensity of an agricultural fire. The RGB and NIR imagery obtained by UAVs can be a good tool to predict the intensity of an agricultural fire, TIR imagery could be used to find mathematical relations between land covers and fire intensity.
Key words: Itinerant agriculture; Agricultural Fire; Drone; Multispectral imagery analyses; Normalized Difference Vegetation Index.

RESUMEN

Antecedentes. La milpa es uno de los sistemas agrícolas tradicionales de Yucatán, México, se realiza mediante el procedimiento agrícola denominado "Roza-tumba-quema". La calidad y la cantidad de combustible forestal (v.g. biomasa) son dos de los principales factores relacionados con la intensidad de la quema. La quema modifica las propiedades del suelo relacionadas con la fertilidad y la producción de cultivos. Se requieren nuevos enfoques para continuar estudiando la importancia del fuego en la agricultura, con la finalidad de mejorar la productividad en los sistemas agrícolas de roza-tumba-quema, tal es el caso de tecnologías de teledetección, como los vehículos aéreos no tripulados (VANTs). **Objetivo.** Analizar el estado de las coberturas del suelo y su influencia en la intensidad de la quema agrícola en el agrosistema "Milpa" mediante el uso de imágenes multiespectrales adquiridas por VANTs. **Metodología.** El sitio de estudio se ubica en el municipio de Tzucacab, Yucatán, México. Se seleccionaron dos parcelas [10-15 y 20-25 años de barbecho], las coberturas del suelo se identificaron y registraron antes y después de la roza-tumba y quema. Se acoplaron sensores multiespectrales [rojo, verde, azul (RGB); infrarrojo cercano (NIR) e infrarrojo térmico (TIR)] en VANTs para obtener imágenes multiespectrales y generar ortomosaicos para su análisis. **Resultados.** Con las imagines multiespectrales, se calculó el Índice de Vegetación

de Diferencia Normalizada [NDVI] y se evaluó su comportamiento espectral. Las imágenes se usaron para analizar la intensidad de la quema. En las imágenes RGB, se observaron patrones de áreas con una mayor cobertura de biomasa seca asociada a una alta intensidad de la quema y áreas con vegetación verde o suelo desnudo asociado a baja intensidad de la quema. Las cubiertas terrestres con alto potencial de combustible mostraron valores bajos de NDVI. **Implicaciones.** El análisis de las imágenes multiespectrales tomadas con drones permiten evaluar rápidamente las coberturas del suelo y la intensidad del fuego en las quemas agrícolas, con las adecuaciones necesarias, en el futuro cercano podría convertirse en una metodología estándar para este tipo de evaluaciones. **Conclusiones.** Este enfoque permitió analizar el estado de las coberturas del suelo para visualmente evaluar la calidad del combustible y su influencia sobre la intensidad de una quema agrícola. Las imágenes RGB y NIR obtenidas por los VANTs pueden ser una buena herramienta para predecir la intensidad de las quemas agrícolas, las imágenes TIR pueden usarse para buscar las relaciones matemáticas entre las coberturas del suelo y la intensidad del fuego.

Palabras clave: Agricultura itinerante; Fuego Agrícola; Dron; Análisis de imágenes multiespectrales; Índice de Vegetación de Diferencia Normalizada

INTRODUCTION

Traditional agricultural techniques from Mayan precolombinan cultures include the burning of the ecosystems followed by a 2-3 years crop cycle and a forest management cycle up to 20 years or more (Mariaca, 2015). However, its use is a controversial topic for scientists and technicians; many authors state that repeated burning is the main cause of yield decrease over time, due to the loss of organic matter, nutrients, and microbial pools, at a point in which the addition of fertilizers cannot help it anymore (Faust & Bilsborrow, 2000; Aguilar et al., 2013; Edem & Udo-Inyan, 2016). The main factors related to burn severity are quality and quantity of forest fuel (v.g. biomass); other important factors are environmental variables such as relative humidity, wind speed and direction and temperature, as well as soil type and moisture (Byram et al., 1952; Sandberg et al., 2001; Hardy, 2005; Hyde et al., 2011; Morfin-Ríos et al., 2012; Rodríguez-Trejo, 2015). It is well known that burning of agricultural residues and stubble have emitted greenhouse gases affecting the ozone layer (IPCC, 2001; Bodí et al., 2012; Stravrakuo et al., 2016). Neary et al. (1999) mention that only 10% of the heat produced during a fire is irradiated downward towards the soil, being this responsible of all changes in soil. Burning also affects the soil mineralogical composition promoting changes in its physical, chemical and biological properties related to soil fertility and crop production (Zabala et al., 2014). Depending on the severity of fire, the changes on the organic matter and soil range from a slight sterilization to protein denaturalization (50–60ºC) until changes in clay mineralogy (950ºC) (Walker et al., 1986), leaving burning products such as mineral grey ashes with little residual C, black carbon with high residual C and other charred substances (Bodí et al., 2014). Slash & burn leads to an increase of C, N, K Ca, Mg and P, many of these ions are lost by erosion (Edén and Udo-Inyan, 2016) with effects in soil up to 10 cm depth after 90 days after burning (Afif Hhouri & Oliveira, 2006). New approaches are needed to continue studying the importance of fire in agriculture to improve productivity in slash & burn agricultural systems. One of these approaches is the use of remote sensing technologies such as UAVs. Many authors have been working with the use of satellite imagery to map burned areas (Zhang et al., 2008; Zha, et al., 2013; Manzo & López, 2013; Liu et al., 2015). Other have studied the severity of the burn, loss of plant coverage and, recovery land rates at different scales across the use specific magnetic spectral bands related to biophysical vegetation features (Miller & Yool, 2002; Díaz-Delgado, 2003; Key & Benson, 2006; De Santis & Chuvieco, 2007; Nieto et al., 2016; Chuvieco et al., 2019; Lizundia-Loiola et al., 2020). Currently, studies about the potential of the imagery taken by UAVs for mapping vegetation stands, assessing biomass, fire intensity, fire effects, forest recovery or building indices (i.e. Excess Greenness Index and the Char Index) are common (Cummings et al, 2017; Fraser et al., 2017; Medvedev, 2019; Pádua et al., 2019; Shin et al., 2019). The objective of this study was to analyze the state of the land covers and its influence on agricultural burning severity, through multispectral imagery (RGB, NIR y TIR) obtained by unattended aerial vehicles (UAVs).

MATERIAL AND METHODS

Study sites

The study sites were two plots located in the Hobonil ranch at the municipality of Tzucacab, Yucatan, Mexico (Figure 1), with north borders to Tixmehuac and Chacsinkín, on south to Quintana Roo state, on the west to Peto and on the east to Tekax. Tzucacab is a calcareous undulated plain, where the main type of soils are Luvisols, climate is subhumid warm with summer rains, average temperature between 24-28 °C and annual precipitation of 1000-1200 mm (INEGI, 2005). The Plot1 had a surface of 263,544.13 m^2 (26.3 ha) with a fallow period of 10-15 years while Plot2 had a surface 39,234.03 m^2 (4 ha) and a fallow period of 20-25 years.
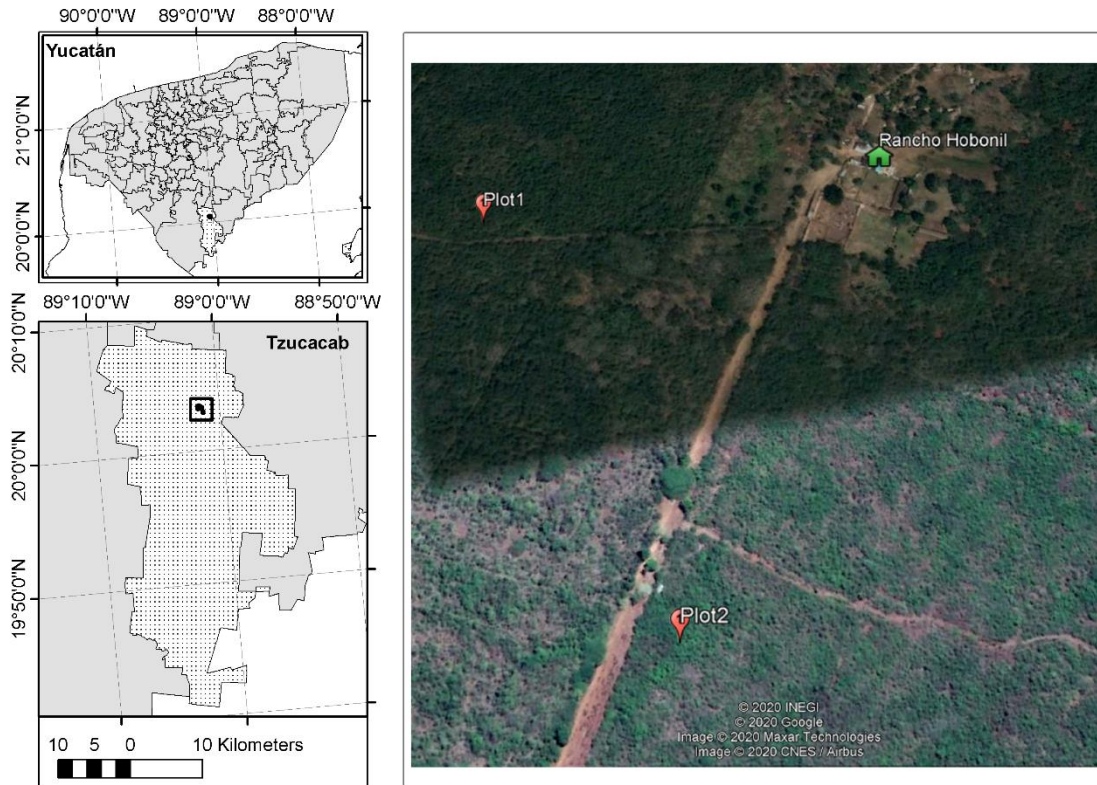
Figure 1. Macro and microlocalization of the study area and studied plots at Hobonil, Tzucabab, Yucatan, Mexico.

Drones and sensors used per studied stage

Three stages of the slash & burn agricultural system were studied: 1) before slash & burn (bS&B), 2) before burn (bB) and 3) after slash & burn (aS&B). In all those stages flights with different UAVs and sensors where performed to obtain multispectral imagery (Table 1).

Flight UAVs plans were developed with the software Pix4DCapture (Pix4D, Prilly, Switzerland) using the following parameters: 1. Flight height: 85 m, 2. Front overlapping: 75 %, 3. Side overlapping: 80 % and, 4. Flight time: 3-5 minutes. Before UAVs

flying, 4 reference marks were placed in the vertices of the plots. When UAVs flights were completed and, imagery files were downloaded, observed and depurated. The following basic photogrammetric processing was realized with the software Agisoft PhotoScan version 1.3 (Agisoft LLC, St. Petersburg, Russia) to produce the following products: image orientation, dense point cloud, mesh and texture, tessera model and orthomosaic. Subsequently, the post-processing to extract the thematic information of interest was carried out. This methodological step was repeated to all images obtained in each of the three studied stages.

Table 1. Drones (UAVs) and sensors used and, flight dates.

Milpa Stage	UAV	Sensor	Plot (day of flight)
bS&B	DJI Phantom 3 Standard	RGB[1]	Plot1 and Plot2 (19/04/2019)
bB	DJI Phantom 4	RGB[1]	Plot1 (06/05/2019), Plot2 (7/05/2019)
	DJI Phantom 4	NIR[2]	Plot2 (7/05/2019)
	DJI Matrice 600	IRT[3]	Plot2 (7/05/2019)
aS&B	DJI Phantom 4	RGB[1]	Plot1 and Plot2 (22/05/2019)
	DJI Phantom 4	NIR[2]	Plot2 (13/05/2019)
	DJI Matrice 600	IRT[3]	Plot1 (13/05/2019)

bS&B= before slash & burn, bB= before burn, aS&B= after slash & burn.
1= Active Pixel Sensor; 2= MAPIR Survey3W with Orange + Cyan + NIR filter; 3= Zenmuse XT 640

Before slash & burn (bS&B) stage

Prior capturing and analyzing the multispectral images, the woody vegetation in each plot was characterized. Ten 10 x 10 m quadrants (100 m^2) were made to obtain a sampling area of 1000 m^2 (0.1 ha). In each quadrant, the height, coverage and diameter at chest height (DCH) of all woody individuals with a DCH ≥1 cm were measured, with these data basal area (BA) was calculated.

This stage represents the current vegetation status, before agricultural activities start. The Geoinformatics procedure used started exporting the RGB orthomosaics of the 2 plots to the software Qgis version 3.6, Noosa. A visual identification of land covers was done, recognizing three classes: Green Biomass (photosynthetic tissue), Dry biomass (Non-photosynthetic tissue) and naked soil (no organic matter). Then a supervised classification was run, using the SCP plugin and the Spectral mapper angle Qgis algorithm, to obtain the spatial zoning and its correspondent statistics.

Before burn (bB) stage

This stage represents a moment where vegetation has been slashed to prepare the site for burning. In this stage RGB, NIR and TIR images were obtained. RGB images were used to calculate the land covers, NIR imagery was used to calculate the NDVI and TIR imagery was used to assess the surface soil temperature.

a. Land cover: RGB Orthomosaics were exported to Qgis and cut to fit the plot size. A visual identification of land covers was done followed by a non-supervised classification. Spatial zoning and its correspondent statistics were obtained.

b. OCN-NDVI: this index was used to analyze the status of the biomass through its reflectivity power using different electromagnetic spectrum bands. Categories were segmented using the spectral values of the OCN filter, which according to the fabricant providing more contrast compared to the RNG filter by reducing the soil interference (https://www.mapir.camera/pages/ocn-filter-improves-contrast-compared-to-rgn-filter). To calculate the index an adaptation of the equation used by Manrique (1999), Díaz (2015) and Fortes *et al*. (2015) was used as indicated in the following expression:

$$NDVI = (\rho R - \rho N) / (\rho R + \rho N)$$

Where:
ρR is the reflectance value of the electromagnetic spectrum red band
ρN is the reflectance value of the electromagnetic spectrum orange band

For the calculation of the OCN-NDVI, the red band (660 nm) was substituted by the orange band (615 nm), whereas the infrared band (850 nm) was substituted by a lower one at 808 nm). The calculations were done by using the bands calculator available in Qgis to obtain a gray tones raster image. Finally, a five categories classification and a Look Up Table (LUT) were generated.

During the burning (dB) stage

Surface temperature

During burning, thermal imagery was taken. Then it was exported to Qgis were interpretation was done by using the rendering tools to create a color lookup table with values from 0-255, where 0 represents the lowest intensity temperature value and 255 the higher intensity temperature value. The temperature readings from the TIR sensor in Plot2 during fire were used to link the highest temperatures to the highest pixel values, temperature of the lowest pixel values (unburnt spots) were assumed equal to the environmental temperature (35°C). All other temperature values were interpolated to build the fire intensity scale.

After slash & burn (aS&B) stage

This stage is right after the burning of vegetation finished. UAV flights where done a few hours after the fire subsided and fumes were naturally dissipated. RGB and NIR imagery were obtained. RGB imagery were used to calculate land cover whereas NIR imagery were used to calculate the spectral NDVI and surface temperature as it was done in previous stages.

RESULTS

Before slash & burn (bS&B) stage

The species composition in the two plots was similar with 27 species being shared between plots. Trees in Plot2 had a total basal area (BA) 2.7 times greater than Plot1. The species with the largest BA in both plots was *Piscidia piscipula* with 3.29 and 12.97 m, for Plot 1 and Plot2, respectively (Table 2). In Plot2 there are 4 species with BA greater than *P. piscipula* in Plot1. In general, shared species between plots have greater BA values in Plot2 compared to Plot1.

The supervised classification shows that green biomass percentage in Plot1 occupied a surface twice as much as that in Plot2, while dry biomass and naked soil covered a greater surface in Plot2 with a more homogeneous distribution compared to Plot1 (Figure 2).

Table 2. The 20 species with the largest basal area in the studied plots in a hectare.

Plot1 (10-15 years)		Plot2 (20-25 years)	
Specie	**Basal area (m2)**	**Specie**	**Basal area (m2)**
Piscidia piscipula (L.) Sarg.	32.9	*Piscidia piscipula* (L.) Sarg.	129.7
Caesalpinia gaumeri (Britton & Rose) Greenm.	27.7	*Bursera simaruba* (L.) Sarg.	72.5
Psidium sartorianum (O. Berg) Nied.	17.0	*Sabal yapa* C. Wright. ex Becc.	45.7
Eugenia foetida Pers.	16.8	*Haematoxylum campechianum* L.	36.0
Diospyros tetrasperma Sw.	15.2	*Acrocomia aculeata* (Jacq.) Lodd. ex Mart.	28.3
Pithecellobium dulce (Roxb.) Benth.	14.5	*Luehea speciosa* Willd.	25.9
Zuelania guidonia (Sw.) Britton & Millsp.	13.2	*Leucaena leucocephala* (Lam.) de Wit. ssp. leucocephala	25.4
Diphysa carthagenensis Jacq.	08.2	*Psidium sartorianum* (O. Berg) Nied.	23.9
Bursera simaruba (L.) Sarg.	06.9	*Zuelania guidonia* (Sw.) Britton & Millsp.	21.5
Caesalpinia yucatanensis (Britton & Rose) Greenm.	06.1	*Lonchocarpus rugosus* Benth.	20.6
Hyperbaena winzerlingii Standl.	05.0	*Diospyros tetrasperma* Sw.	17.4
Colubrina arborescens (Mill.) Sarg.	05.0	*Ehretia tinifolia* L.	17.3
Leucaena leucocephala (Lam.) de Wit. ssp. leucocephala	04.9	*Pithecellobium dulce* (Roxb.) Benth.	17.0
Swartzia cubensis (Britton & Wills) Standl. var. cubensis	04.8	*Eugenia foetida* Pers.	16.2
Esenbeckia pentaphylla (Macfad.) Griseb.	03.6	*Diphysa carthagenensis* Jacq.	14.7
Harpalyce rupícola Donn. Sm.	03.5	*Chloroleucon mangense* (Jacq.) Britton & Rose. var. leucospermum (Brandegee) Barneby & Grimes.	12.9
Rehdera trinervis (S.F. Blake) Moldenke.	03.4	*Guazuma ulmifolia* Lam.	12.3
Ficus crocata (Miq.) Miq.	03.2	*Machaonia lindeniana* Baill.	12.1
Lonchocarpus punctatus Kunth.	03.1	*Havardia albicans* (Kunth) Britton & Rose.	10.1
Sideroxylon persimile (Hemsley) Pennington ssp. Persimile	03.0	*Cordia alliodora* (Ruiz & Pav.) Oken.	09.6
Sum of all other 23 species	33.2	*Sum of all other 26 species*	67.5
TOTAL	232.4		636.7

Before burn (bB) stage

Land covers

Four classes of land cover were identified in each plot but being distinct from each other (Figure 3). In Plot1 identified classes were: 1) Green biomass (alive not cut vegetation), 2) Dry biomass (mostly leaves and branches), 3) Trunks (cut-down trunks) and, 4) semi-dried biomass (not completed dry leaves and branches). In Plot2 the identified 5 classes were: 1) Naked soil (no biomass atop), 2) Green biomass, 3) Dried biomass; 4) Semi-dried biomass y 5) Trunks. The classified images show two times more surface occupied by green biomass in Plot2 with a more uniform distribution than Plot1. The dry biomass occupies a third of the surface in Plot2 with a distribution concentrated in the northern part of the plot. In Plot1 dry biomass occupies almost 50% of the plot with a more uniform distribution. Green Biomass (representing uncut vegetation) was 3 times greater in Plot1 compared to Plot2. Plot2 had 6%

more trunks than Plot1. Semidried biomass was similar in both plots.

Vegetation index

The calculated OCN-NDVI for Plot2 shows values ranging from -0.25 to 0.54 (Figure 4). Values for this index range from -1 to 1, where -1 represent dead plants or inanimate objects and 1 represents very healthy vegetation (Viana-Soto *et al*., 2017). Lowest values are located in the north, whereas the highest values are located in the south part of the plot. NDVI not was calculated for Plot1.

During the burning (dB) stage

Surface temperature

Surface temperature values in Plot1 ranged from 35-455°C, the first value corresponding to unburnt sites and the last one to the maximum intensity fire sites (Figure 5). The majority of the plot reached values

greater than 86°C but some scattered regions of low and high temperatures are present.

The TIR image of Plot2 shows that burn was not distributed homogenously (Figure 6). The higher fire intensities were only reached in 22% of the plot surface, 52% of the surface had low fire intensities and the rest had intermediate intensity values. Contrary to our expectations, this pattern was not related to the pattern observed for the OCN-NDVI index. Factor such as level of biomass dryness and/or wind currents during burning could explain this.

After slash & burn (aS&B) stage

Land covers

The non-supervised classifications of both plots show a non-uniform burning event with a great surface of un-burnt trunks and branches (Figure 7). In Plot2 the burnt surface and the surface with burnt trunks and branches were 1.4 times and 2.3 times greater than in Plot1. In Plot1, 5 categories were identified, while in Plot2 only 4. In Plot1 20% of the land cover was green biomass and 25.2% was unburnt naked soil, suggesting areas were burning was not effective. A bigger ash surfaces presented on Plot2 supports this idea.
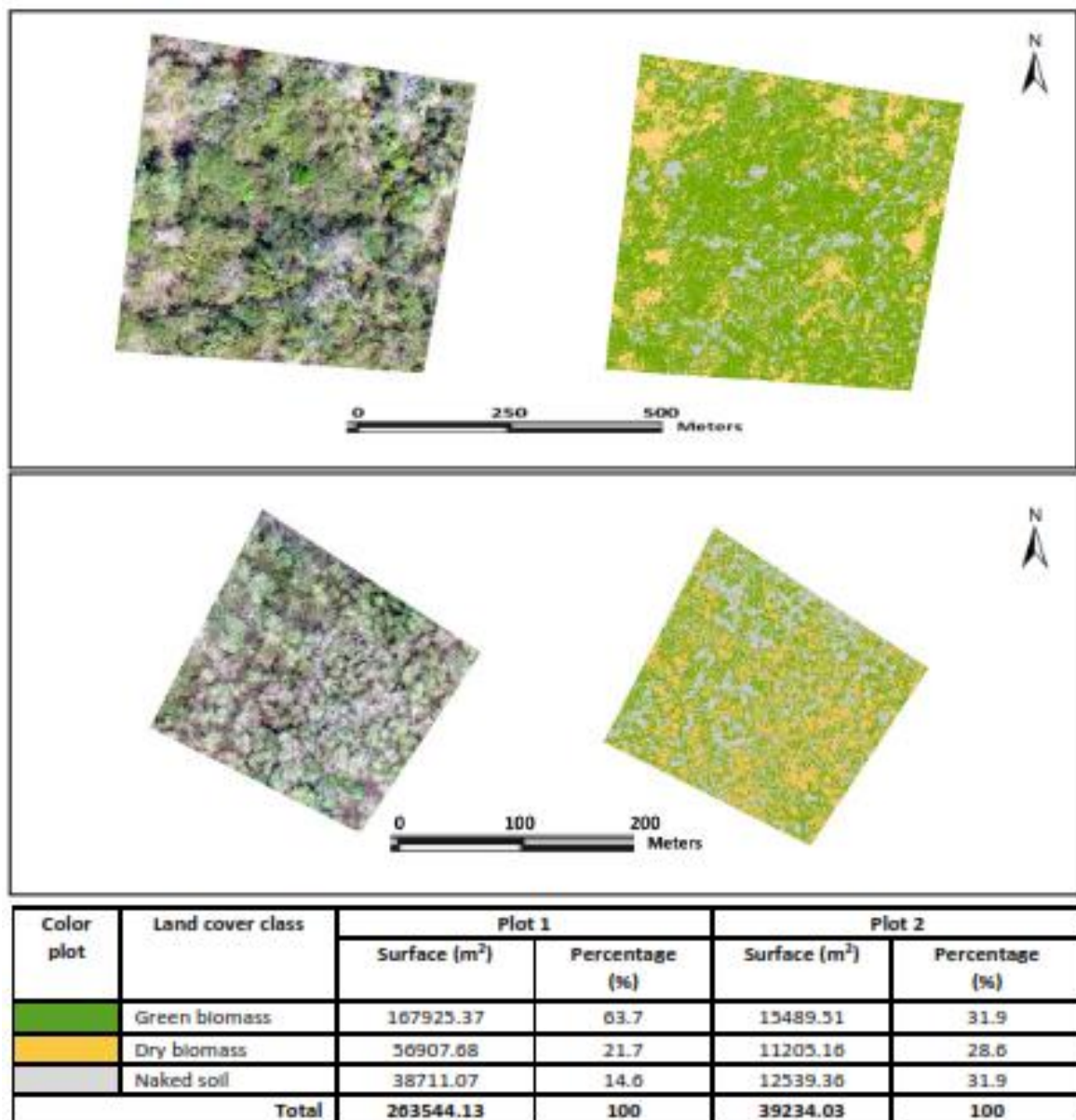

Color plot	Land cover class	Plot 1		Plot 2	
		Surface (m²)	Percentage (%)	Surface (m²)	Percentage (%)
	Green biomass	167925.37	63.7	15489.51	31.9
	Dry biomass	56907.68	21.7	11205.16	28.6
	Naked soil	38711.07	14.6	12539.36	31.9
Total		263544.13	100	39234.03	100

Figure 2. Land covers of Plot1 (10-15 years of fallow) and Plot2 (20-25 years of fallow) before slash & burn. Up: RGB image and supervised classification of Plot1. Middle: RGB image and non-supervised classification of Plot2. Down: land cover statistics of both plots according to their classifications.

Plot 1					Plot 2			
Color plot	Land cover class	Surface (m²)	Percentage (%)		Color plot	Land cover class	Surface (m²)	Percentage (%)
	Green biomass	15891.71	6.03			Naked soil	941.62	2.4
	Dry biomass	130586.09	49.55			Green biomass	5296.59	13.5
	Trunks	30096.74	11.42			Semi-dried biomass	12358.72	31.5
	Semi-dried biomass	86969.56	33.0			Dried biomass	13771.14	35.1
	Total	263544.13	100			Trunks	6865.96	17.5
						Total	39234.03	100

Figure 3. Land covers of Plot1 (10-15 years of fallow) and Plot2 (20-25 years of fallow) before burn. Up: RGB image and supervised classification of Plot1. Middle: RGB image and non-supervised classification of Plot2. Down: land cover statistics of both plots according to their classifications.
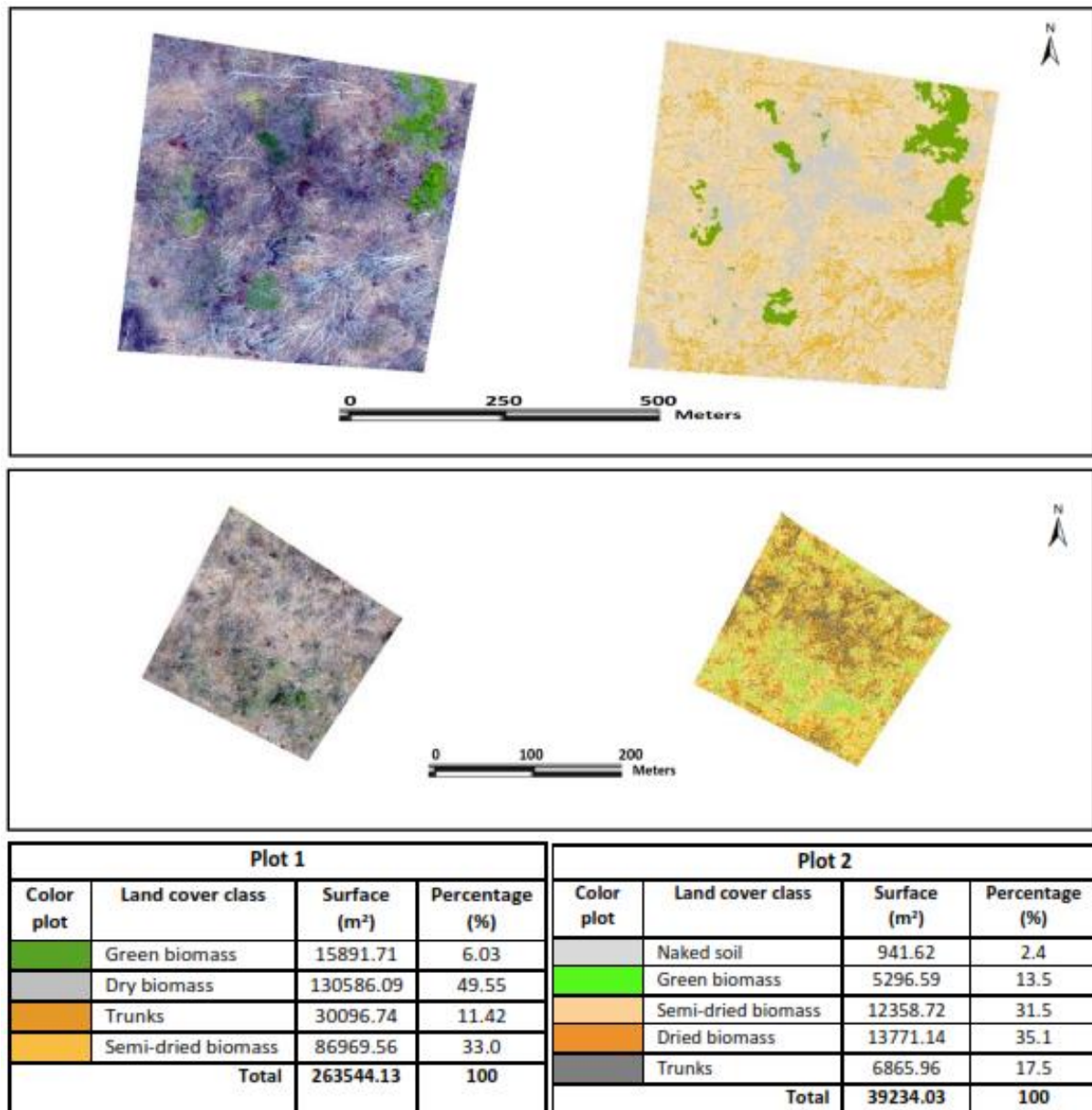
DISCUSSION

Before slash & burn (bS&B) stage

The characterization of the vegetation showed greater basal area values in Plot2, suggesting a bigger amount of accumulated biomass in the 20-25 years old forest and therefore, a better stock of fuel for burning compared to Plot1. Analyses of RGB imagery allowed the identification and quantification in detail of the land covers in this stage by using mapping units smaller than those usually obtained from high-resolution satellite images. Hernández Gómez *et al*. (2020) had good results on identifying logging impacts in a forest by using LANDSAT 8 images but concluded that a greater imagery resolution is needed for better accuracy. In this study, the greater resolution of the images allowed a clearly distinction of features, the selection of training seeds and the use of supervised classifications.

Regarding the methodology to study the slash & burn agriculture by using multispectral imagery, two phases (basic photogrammetric process and information extraction) and three transversal moments were observed (before slash & burn, after slash & burn and post burn). A long-term study is desirable and should include the crop growth and yield as well as the vegetation growth analyses over the fallow period. This approach can also be applied to other similar situations such as forest fires just changing the moments of study.
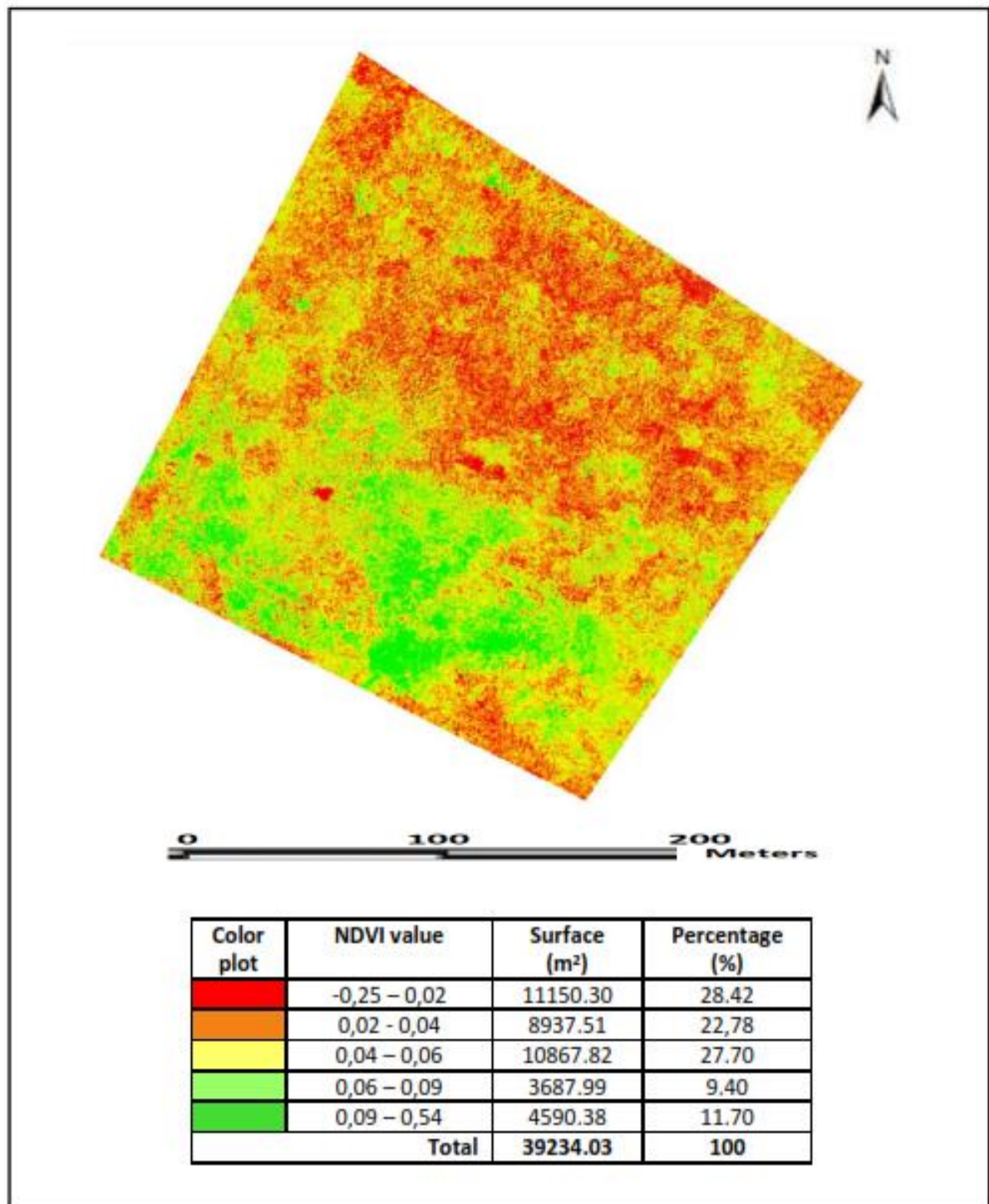
Color plot	NDVI value	Surface (m²)	Percentage (%)
	-0,25 – 0,02	11150.30	28.42
	0,02 - 0,04	8937.51	22,78
	0,04 – 0,06	10867.82	27.70
	0,06 – 0,09	3687.99	9.40
	0,09 – 0,54	4590.38	11.70
	Total	39234.03	100

Figure 4. NDVI image of Plot2 built with NIR sensor.

The greater surface of green biomass observed in Plot1is related to the age of the vegetation presenting young trees with a canopy not well developed, promoting a denser vegetation coverage compared to Plot2 where trees are bigger and more disperse (Melo-Cruz *et al*., 2012; Hernández *et al*., 2013). This dispersion also explains the greater amount of naked soil spots in Plot2. The greater biomass (green + dry) surface in this plot, suggests better opportunities to have a more intense fire here. However, still the quantification of the biomass in plots is needed; since thickness of biomass layer can vary across the plots.

Before burn (bB) stage

RGB imagery analyses allow identifying land cover classes but not biomass volumes. In this sense, other methods or processing techniques are needed to obtain this important parameter associated to the available amount of fuel. Recently, d'Oliveira *et al*. (2020) published a methodology to estimate aboveground biomass in dense forests by using

UAVs imagery and the dense point clouds approach; authors found similar aboveground biomass results to those obtained by using LANSAT imagery. The high resolution of the UAV images not only allow the clear identification and measurement of trunks but also the distinction between green biomass and semidried biomass. In this stage, non-supervised classifications were used because the overlapping of the different plant tissues make difficult to separate their spectral firms. In this case, the high resolution of the images was not useful as they had too many different pixel levels causing the identification of too many covers. To solve this problem, the use of sample selection methods should be investigated to achieve more accurate classification at sub-pixel levels (Pu, 2008).

Land covers

The fallow period in each plot explains the different land cover categories found. In Plot2 where vegetation is older, more uncut trees were left in the field; this is a common practice among farmers to save important tree species to be used in the future. The green biomass in Plot2 was greater because the slashing of the vegetation was done later here than in Plot1; besides older vegetation in Plot2 showed thicker branches, which takes a longer time to dry. In Plot2 the distribution of the different land cover classes was related to the presence of located tree stands, whereas in Plot1 the vegetation distribution was more homogeneous.
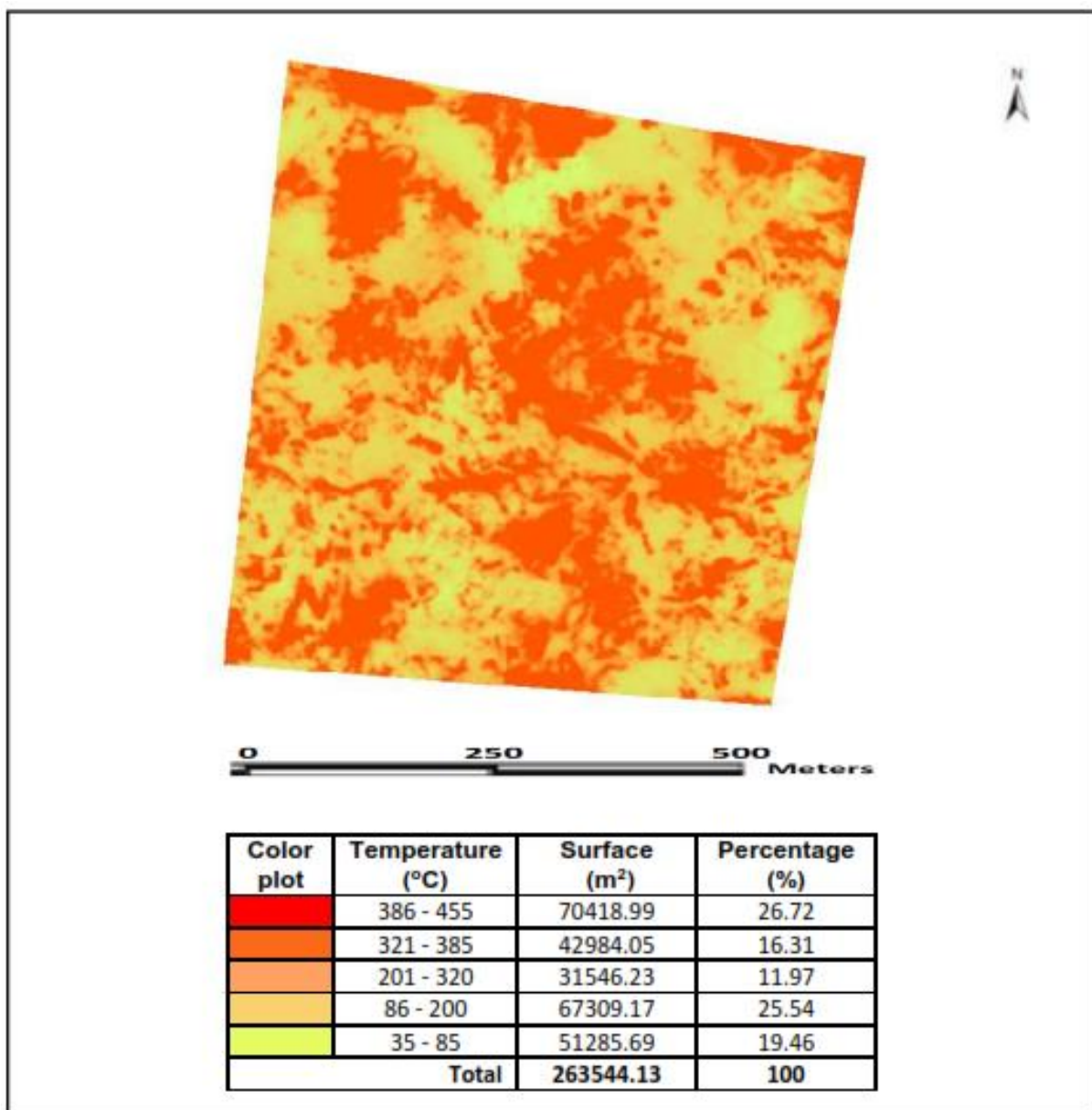

Color plot	Temperature (°C)	Surface (m²)	Percentage (%)
	386 - 455	70418.99	26.72
	321 - 385	42984.05	16.31
	201 - 320	31546.23	11.97
	86 - 200	67309.17	25.54
	35 - 85	51285.69	19.46
	Total	263544.13	100

Figure 5. Surface temperature in Plot1. Up: Thermic image. Down: Identified temperature levels and surfaces.

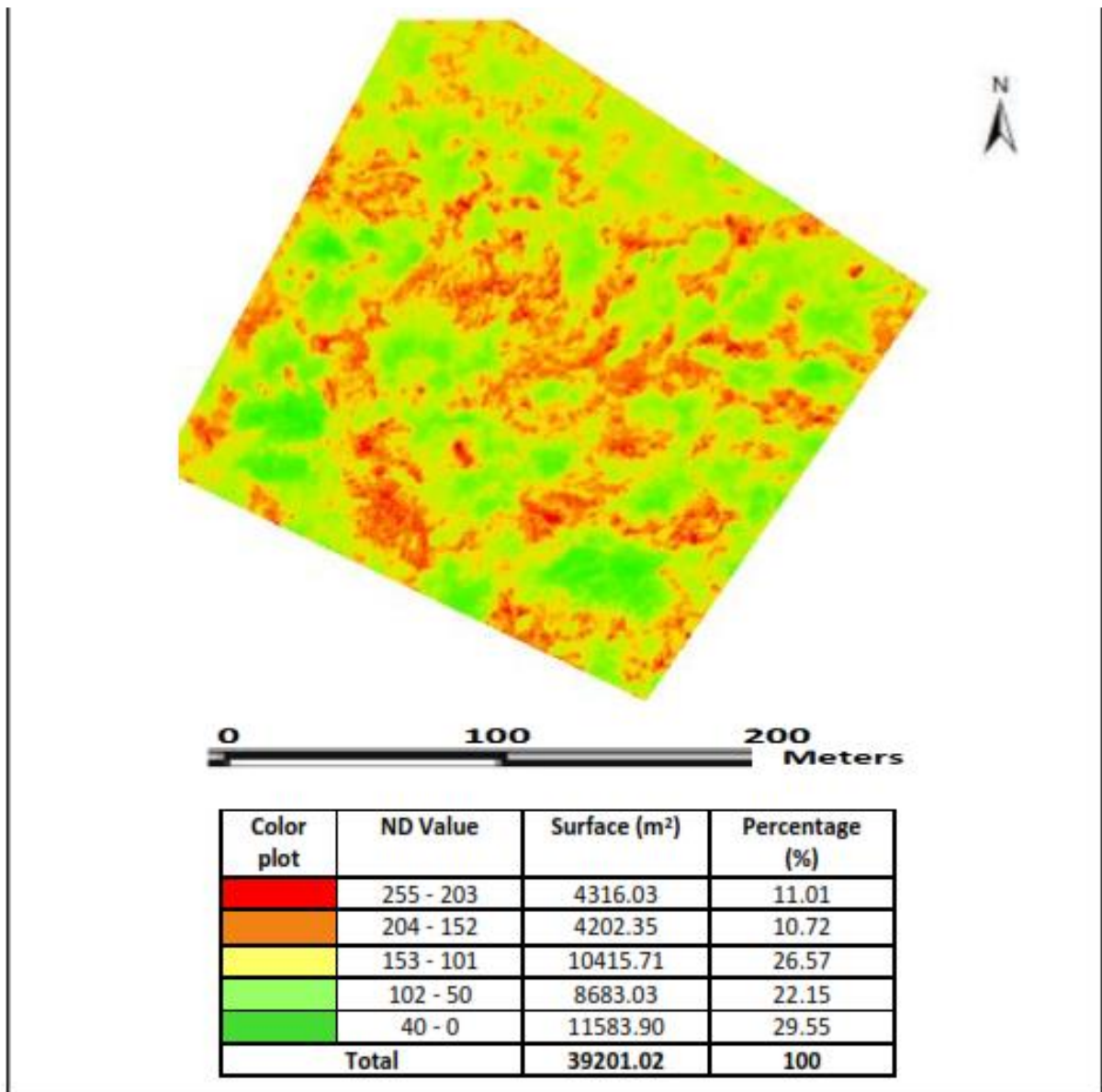| Color plot	ND Value	Surface (m²)	Percentage (%)
	255 - 203	4316.03	11.01
	204 - 152	4202.35	10.72
	153 - 101	10415.71	26.57
	102 - 50	8683.03	22.15
	40 - 0	11583.90	29.55
Total		39201.02	100

Figure 6. Thermic image of Plot2 and levels of temperature. Red color is the highest level of Surface temperature.

Vegetation Index

Low OCN-NDVI values in Plot2 are associated to areas with accumulations of dry biomass or naked soil (no photosynthetic activity); in this sense, values under 0.04 represent the areas with the greater combustion potential (Nieto *et al*., 2017). OCN-NDVI values ranging from 0.04 to 0.06 represent the transition between photosynthetic and no photosynthetic activity. OCN-NDVI values higher than 0.06 represent mostly alive vegetation although cut branches with alive leaves could be also been represented.

Surface temperature

Although the lack of homogeneity of the burning in Plot2 can be related to the distribution of the vegetation and biomass on the surface, there was a coincidence between the highest temperature points with the presence of trunks and dry branches. Other factors such as the surface of naked soils, amount and level of the biomass dryness and, changes in wind direction during the burn, could have influence on surface temperature.

After slash & burn (aS&B) stage

The high contrast of the RGB imagery allowed to classify the land covers after burning. Burnt features were clearly separated from the matrix. However, it was not possible to assess the volumes of incinerated materials. In order to improve this a 3D image processing approach is suggested (Escalante *et al*., 2016; Botello *et al*., 2019).
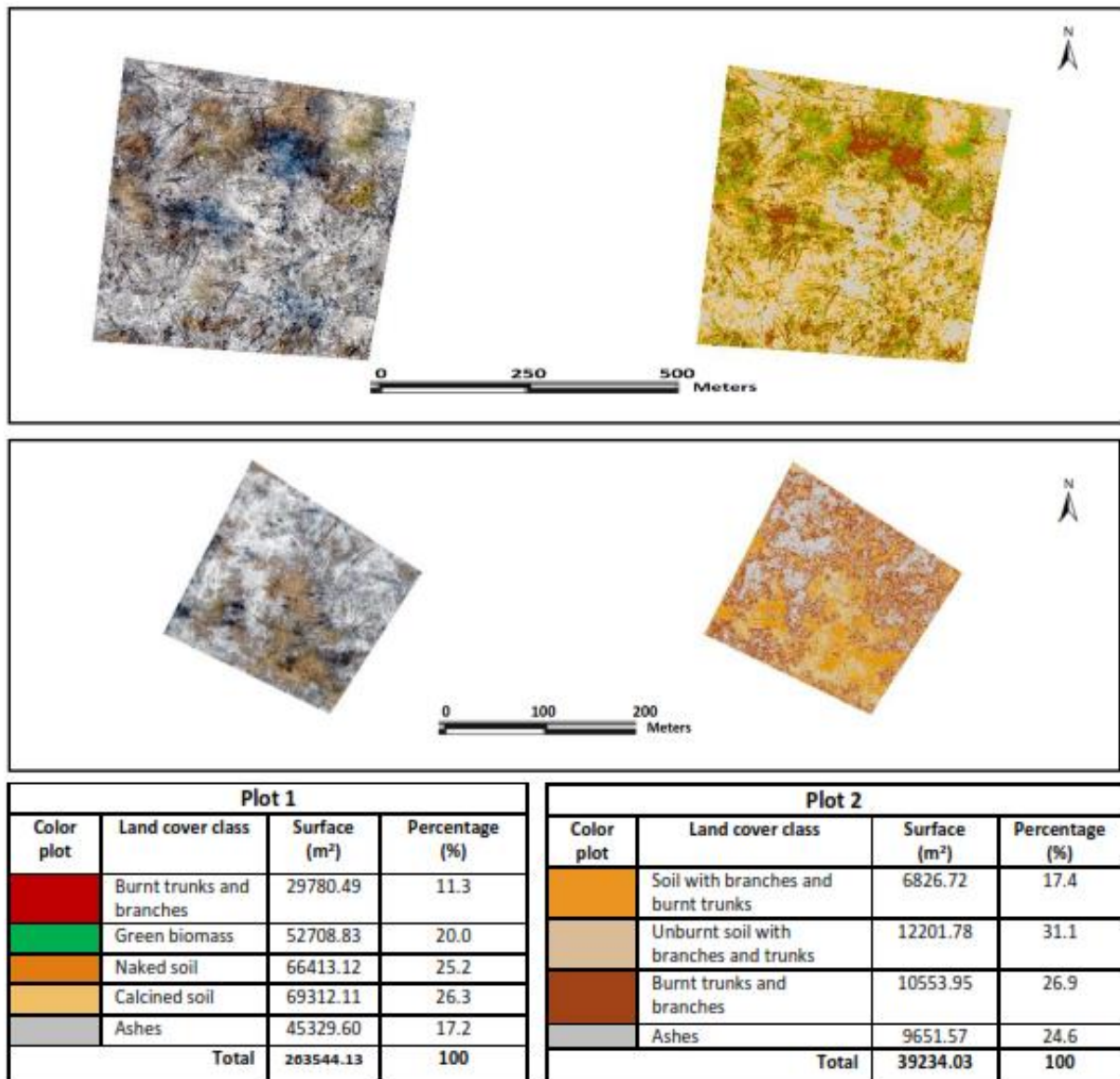
Plot 1			
Color plot	Land cover class	Surface (m²)	Percentage (%)
	Burnt trunks and branches	29780.49	11.3
	Green biomass	52708.83	20.0
	Naked soil	66413.12	25.2
	Calcined soil	69312.11	26.3
	Ashes	45329.60	17.2
	Total	263544.13	100

Plot 2			
Color plot	Land cover class	Surface (m²)	Percentage (%)
	Soil with branches and burnt trunks	6826.72	17.4
	Unburnt soil with branches and trunks	12201.78	31.1
	Burnt trunks and branches	10553.95	26.9
	Ashes	9651.57	24.6
	Total	39234.03	100

Figure 7. Land covers on Plot1 and Plot2 after burning. Top: RGB image (left) and non-supervised classification (rigt) of Plot1. Middle: RGB image (left) and non-supervised classification (right) of Plot2. Down: land covers statistics of both plots according to the non-supervised classification.

The highest fire intensity values were related to areas with high rates of combustion. However, contrary to our expectations, these values do not match with NDVI low values which are normally related to areas where low photosynthetic activity is present (i.e. burnt biomass). We suspect of an incorrect calibration of the camera.

This is one of the first studies in Mexico were slash & burn agriculture is studied by analyzing multispectral drone images. We utilize the visible (RGB), infrared (NIR) and thermic (TIR) sensors. Other sensors are recommended in order to be able to calculate indexes such as the Normalized Burn Ratio –NBR-, Normalized difference moisture index–NDVI-, etc.) (Mustafa *et al.*, 2017). A thermographic sensor is also desirable to record surface temperatures during burning events. In the future, it is probably that commercial drones have all

these sensors on board. In fact, DJI just release a 5 multispectral camera drone for agriculture purposes (https://www.dji.com/p4-multispectral).

The bigger burnt surface identified in Plot2 is related to the presence of thick fallen trunks and the higher number of branches observed, this represent a better quality fuel biomass. However, in some parts of the plot many not-well burnt trunks were also observed suggesting that intensity of fire was not enough. In Plot1 the lower burnt surface is related to areas with naked soils, thin layers of litter and low amounts of trunks and branches. Litter and weeds burned easily but branches and trunks were only partially burned. One week before burning there was a light rain event that although did not influence the dryness of the biomass it could influence the soil moisture, preventing a better burning.

During burning (dB) stage

Surface temperature

There is no relation between the soil surface with land covers observed in RGB image, high temperatures (321 and 455 ºC) are related to areas with more surface of dry biomass and trunks. Areas with values between 35 and 40 ºC correspond to areas where there was no burning al all, mainly naked soil. Images show that fire was similar in both plots following a patchy pattern with no apparent relation to the biomass present in the plots. However, green biomass and/or outcrops can be features limiting the even burning in the plots.

CONCLUSIONS

The imagery collected by means of VANTs allowed to analyze the state of land covers to visually assess the quality of fuel and its influence on the intensity of an agricultural fire in a Milpa agrosystem. The RGB and NIR imagery obtained by UAVs can be a good tool to predict the intensity of an agricultural fire, TIR imagery could be used to find mathematical relations between land coverages to fire intensity.

Competing interests: The authors have declared that no competing interests exist.

Compliance with ethical standards: The authors declare compliance with ethical standards.

Data availability: Metadata is available with Dámaso R. Ponvert-Delisles Batista [damaso.ponvert@gmail.com] upon reasonable request.

REFERENCES

Aguilar, B., Carrancho, A., Gogichaishvili, A., Quintana, P., Bautista, F., Morales, J., Faust, B. 2013. Influence of agricultural burning on magnetic properties in Maya milpas. Latinmag Letters. 3:(2013)OD08:1-4. Proceedings Montevideo, Uruguay.

Bodí, M.B., Cerdà, A., Mataix-Solera, J., Doerr, S.H. 2012. Efectos de los incendios forestales en la vegetación y el suelo en la cuenca mediterránea: revisión bibliográfica. Boletín de la Asociación de Geógrafos Españoles 58:33-55. ISSN: 0212-9426.

Bodí, M.B., Martin, D.A., Balfour, V.N., Santín, C., Doerr, S.H., Pereira, P., Cerdà, A., Mataix-Solera, J. 2014. Wildland fire ash: Production, composition and eco-hydro-geomorphic effects. Earth-Science Reviews. 130:103-127. DOI: 10.1016/j.earscirev.2013.12.007.

Botello, C., Gavi, F., Tijerina, L., Galvis, A., Roblero, R. 2019. Estimación de biomasa aérea de forrajes de invierno bajo riego a través de un dron. Agroproductividad. 12(4):25-31.

Brown, S. 1996. Tropical forests and the global carbon cycle: estimating state and change in biomass density. In: Apps, M.J., Price, D.T. (Eds.), Forest Ecosystems, forest management and the global carbon cycle. Springer, Berlin. pp. 13-44.

Byram, G.M., Fons, W.L., Sauer, F.M., Arnold, P.K. 1952. Thermal properties of forest fuels (Interim Technical Report 404 for AFSWP). Berkeley, California: Division of Fire Research. U.S. Department of Agriculture.

Chuvieco, E.; Mouillot, F.,van der Werf, G.R., San Miguel, J., Tanasse, M., Koutsias, N., García, M., Yebra, M., Padilla, M., Gitas, I., Heil, A, Hawbaker, T.J., Giglio, L. 2019. Historical background and current developments for mapping burned area from satellite Earth observation. Remote Sensing of Environment. 225:45–64.

Cummings A.R., Karale Y., Cummings G.R., Hamer E., Moses P., Norman, Z., Captain, V. 2017. UAV-derived data for mapping change on a swidden agriculture plot: preliminary results from a pilot study. International Journal of Remote Sensing, 38:8-10, 2066-2082. DOI: 10.1080/01431161.2017.1295487

d'Oliveira M., Broadbent E., Oliveira L. Almeida D., Papa D., Ferreira M., Almeyda-Zambrano A., Silva C., Avino, F., Prata G., Mello, R., Figueiredo E., de Castro, L., Junior, L. Albuquerque, R., Brancalion, P., Wilkinson, B., Oliveira-da Costa, M. 2020. Aboveground biomass estimation in Amazonian tropical forests: a comparison of Aircraft- and GatorEye UAV-borne LiDAR Data in the Chico Mendes Extractive Reserve in Acre, Brazil. Remote Sens. 12(11), 1754. DOI: 10.3390/rs12111754

De Santis, A., Chuvieco, E. 2007. Burn severity estimation from remotely sensed data:

performance of simulation versus empirical models. Remote Sensing of Environment. 108:422-435. DOI: 10.1016/j.rse.2006.11.022.

Díaz, J.J. 2015. Estudios de índices de vegetación a partir de imágenes aéreas desde UAS/RPAS y aplicaciones de estas a la agricultura de precisión. Trabajo de Fin de Master. 2014-2015, Universidad Complutense de Madrid, Madrid, España. 78 pp.

Díaz-Delgado, R. 2003. Efectos de la recurrencia de los incendios sobre la resiliencia pos incendio de las comunidades vegetales de Cataluña a partir de imágenes satélite. Ecosistemas XII (3).

Duarte, C.M. 2006. Cambio Global. Impacto de las actividades humanas sobre el sistema tierra. Consejo Superior de Investigaciones Científicas (CSIC), España, 170 p..

Edem, I.D., Udo-Inyang, U.C. 2016. Critical Issues of Agricultural Burning on Soil Health and Atmospheric Greenhouse Gases (GHGs) Concentration. Research Journal of Water, Soil and Air Pollution. 2(1):1-10.

Escalante, J.O., Cáceres, J.J., Porras, H. 2016. Ortomosaicos y modelos digitales de elevación generados a partir de imágenes tomadas con sistemas UAV. Tecnura. 20(50):119-140. DOI: 10.14483/udistrital.jour.tecnura.2016.4.a09 .

Faust, B., Bilsborrow, R.E. 2000. Maya culture, population and the environment in the Yucatan Peninsula. *In* Wolfgang Lutz, Warren Sanderson, and Lionel Prieto, eds., Population, Development and the Environment in the Yucatan Peninsula from Ancient Maya to 2030, Luxemburg, Austria: International Institute for Applied Systems Analysis, (RR 00-14): 73-107.

Fortes, R., Prieto, M.H., García-Martín, A., Córdoba, A., Martínez, L., Campillo, C. 2015. Using NDVI and guide sampling to develop yield prediction maps of processing tomato crop. Spanish Journal of Agricultural Research. 13(1):1-9.

Fraser, R.H., van der Sluijs, J., Hall, R.J. 2017. Calibrating Satellite-Based Indices of Burn Severity from UAV-Derived Metrics of a Burned Boreal Forest in NW. Canada. Remote Sens. 9: 279-286. DOI:10.3390/rs9030279

Giardina, C.P., Sanford, R.L., Dockersmith, I.C. 2000. Changes in soil phosphorus and nitrogen during slash-and-burn clearing of a dry tropical forests. Soil Science Society of America Journal. J 64:399–405. DOI: 10.2136/sssaj2000.641399x

Granados, D., López, G.F., Trujillo, E. 1999. La milpa en la zona maya de Quintana Roo. Revista de Geografía Agrícola. 28:57-72.

Hardy. C.C. 2005. Wildland fire hazard and risk: Problems, definitions and context. Forest ecology and management. 211:73-82. DOI: 10.1016/j.foreco.2005.01.029

Hernández, A., Schwendter, O., Arrechea, E., Forcadell, J.M., Guinart, D., Vela, A., Vayreda, J., Comas, L., Camprodón, J., García, O., Eduard, E., Atauri, J.A. 2017. El papel de los bosques maduros en la conservación de la biodiversidad. Ed. Fundación Fernando González Bernáldez, Madrid. EUROPARC-España. 52 pp.

Hernández-Gómez I.U., Vazquez-Luna D., Cerdan-Cabrera C.R., Navarro-Martinez A., Ellis E. A. 2020. Mapping disturbance from selective logging in tropical forests of the Yucatan Peninsula, Mexico. Tropical and Subtropical Agroecosystems 23 (1) 1-19.

Hernández-Xolocotzi, E., Arias, L.M., Pool, L. 1994. El sistema agrícola de roza-tumba-quema en Yucatán y su capacidad de sostenimiento. En: Rojas Rabiela T, (coord.), Agricultura indígena: pasado y presente. CIESAS, México, D.F., pp. 343-358.

Hernández-Xolocotzi, E., Bello, E., Bello, S. 1995. La milpa en Yucatán. Un sistema de Producción agrícola tradicional, Tomo 1. Editorial Talleres Gráficos del Colegio de Postgraduados. 287 pp.

Hernández-Xolocotzi, E., Bello, E., Bello, S. 1995. La milpa en Yucatán. Un sistema de Producción agrícola tradicional, Tomo 2. Editorial Talleres Gráficos del Colegio de Postgraduados. 300 pp.

Hyde, J.C., Smith, A.M.S., Ottmar, R.D., Alvarado, E.C., Morgan, P. 2011. The combustion of sound and rotten coarse woody debris: a review. International Journal of Wildland Fire. 20:163–174. DOI: 10.1071/WF09113

INEGI. 2005. Prontuario de información geográfica municipal de los Estados Unidos Mexicanos Tzucacab, Yucatán, Fuente: INEGI. Marco Geoestadístico Municipal 2005. Versión 3.1. Información Topográfica Digital Escala 1:250 000 serie II y serie III. 9 pp.

IPCC. 2001. Climate Change 2001. The scientific basis. Inter-Government Panel on climate change. Cambridge Univ. Press, U.K. 867 pp.

Key, C.H., Benson, N.C. 2006. Landscape Assessment (LA). Sampling and Analysis Methods. En FIREMON: Fire effects monitoring and inventory system. Ed D. Lutes, R. United States Department of Agriculture, Forest Service, Rocky Mountain Research Station General Technical Report RMRS-GTR-164-CD. pp: 1-58.

Khouri, E.A., Oliveira, J.A., 2006. Efectos del fuego prescrito sobre matorral en las propiedades del suelo. Investigacion Agraria: Sistemas y Recursos Forestales 15(3):262-270.

Landon S. & Van Rees K. 2020. Assessment of residual slash coverage using UAVs and implications for aspen regeneration. Journal of Unmanned Vehicle Systems 8(1): 19-29. DOI: 10.1139/juvs-2019-0001

Lara, E., Caso, L., Aliphat, M. 2012. El sistema milpa roza, tumba y quema de los Maya Itzá de San Andrés y San José, Petén Guatemala. Ra Ximhai 8(2):71-92.

Liu, M., Song, Y., Yao, H., Kang, Y., Li, M., Huang, X. 2015. Estimating emissions from agricultural fires in the North China Plain based on MODIS fire radiative power. Atmos. Environ. 112:326–334. DOI: 10.1016/j.atmosenv.2015.04.058

Lizundia-Loiola J., Pettinari M. L., Chuvieco E. 2020. Temporal Anomalies in Burned Area Trends: Satellite Estimations of the Amazonian 2019 Fire Crisis. Remote Sensing 2020, 12(1), 151. DOI: 10.3390/rs12010151

Manrique, E.G. 1999. Índices de Vegetación. Aplicación del NDVI. Teledetección. Avances y Aplicaciones, VIII Congreso Nacional de Teledetección, Albacete, España, pp: 217-219.

Manzo, L., López, J. 2013. Detención de áreas quemadas en el sureste de México, utilizando índices pre y post - incendio NBR y BAI, derivados de compuestos MODIS. Revista Internacional de Ciencia y Tecnología de la Información Geográfica. 2(13):66-83.

Mariaca, R. 2015. La milpa maya yucateca en el siglo XVI: Evidencias etnohistóricas y conjeturas. Etnobiología. 13(1):1-25.

Martín-Castillo, M. 2016. Milpa y capitalismo: opciones para los campesinos mayas yucatecos contemporáneos. LiminaR. Estudios Sociales y Humanísticos. 14(2):101-114.

Medvedev A., Telnova N., Kudikov A. 2019. Highly-detailed remote sensing monitoring of tree overgrowth on abandoned agricultural lands. Forest Science Issues 2(3): 1-12.

Melo-Cruz, O., Rodríguez-Santos, N., Rojas-Ramírez, F. 2012. Patrones de arquitectura foliar asociados al crecimiento funcional de cinco especies leñosas nativas de la cordillera oriental utilizadas en restauración ecológica en la sabana de Bogotá. Colombia Forestal 15(1):119 – 130.

Miller, J.D., Yool, S.R. 2002. Mapping Forest post-fire canopy consumption in several overstory types using multi-temporal Landsat TM and ETM data. Remote Sensing and Environment. 82:481-496. DOI: 10.1016/S0034-4257(02)00071-8.

Morfin-Ríos, J.E., Jardel, E.J., Alvarado, C., Michel-Fuentes, J.M. 2012. Caracterización y cuantificación de combustibles forestales. Comisión Nacional Forestal-Universidad de Guadalajara. Guadalajara, Jalisco, México. 59 pp.

Moya, X., Caamal, A., Ku, B., Chan, E., Armendáriz, I., Flores, J., Moguel, J., Noh, M., Rosales, M., Xool, J., 2003. La agricultura campesina de los mayas en Yucatán. Leisa, Revista de Agroecología. 19(0):7-17.

Mustafafa, M.T., Hassoon, K.I., Hussain, H.M., Abd, M.H. 2017. Using water indices (NDWI, MNDWI, NDMI, WRI and AWEI) to detect physical and chemical parameters by apply remote sensing and GIS techniques. International Journal of Research–Granthalayah. 5(10):117-128.

Neary, D.G., Klopatek, C.C., DeBano, L.F., Folliott, P.F. 1999. Fire effects on belowground sustainability: A review and synthesis. Forest ecology and management 122:51–71.

Nieto, A., Navazo, G., Moreno, G. 2016. Análisis de incendios forestales mediante Sistemas de Información Geográfica y Teledetección. Estudio de caso en Sierra de Gata (2015). En: Tecnologías de la Información Geográfica en el Análisis Espacial. Aplicaciones en los Sectores Público, Empresarial y Universitario. pp: 247-268.

Nieto, A., Navazo, G., Moreno, G. 2017. Delimitación y análisis del incendio forestal de Sierra de Gata (Cáceres) mediante imágenes de los satélites Landsat 8 y Sentinel 2. 7mo. Congreso Forestal Español, Sociedad Española de Ciencias Forestales, Extremadura, España, 7CFE01-451, 12 pp.

Pádua, L., Adão, T., Guimarães, N., Sousa, J.J., Peres, C.E., Sousa, A. 2019. Post-fire forestry recovery monitoring using high-resolution multispectral imagery from

unmanned aerial vehicles. International Archives of the Photogrammetry, Remote Sensing & Spatial Information Sciences. Spatial Inf. Sci., XLII-3/W8, 301–305, http://dx.doi.org/10.5194/isprs-archives-xlii-3-w8-301-2019

Pool, L. 2001. Dinámica de la milpa en Yucatán: Una experiencia de investigación participativa. ECOfronteras 13:26-28.

Pu, R., Gong, P., Michishita, R., Sasagawa, T. 2008. Spectral mixture analysis for mapping abundance of urban surface components from the Terra/ASTER data. Remote Sensing of Environment. 112(3): 939-954. DOI: 10.1016/j.rse.2007.07.005

Razo-Zárate, R, Gordillo-Martínez, A.J., Rodríguez-Laguna, R., Maycotte-Morales, C., Otilio, Acevedo-Sandoval, O.A. 2013. Estimación de biomasa y carbono almacenado en árboles de oyamel afectados por el fuego en el Parque nacional "el chico", Hidalgo, México. Madera y Bosques 19(2): 2013:73-86.

Re, A. 1996. The Two Milpas of Chan Kom. Scenarios of a Maya Village Life. State University of New York Press, Albany. 211 pp.

Rodríguez-Trejo, D.A. 2015. Incendios de vegetación: su ecología, manejo e historia. Vol. 2. Guadalajara, Jalisco, México: Biblioteca Básica de Agricultura.

Sandberg, D.V., Ottmar, R.D., Cushon, G.H. 2001. Characterizing fuels in the 21st century. International Journal of Wildland Fire. 10(3 and 4):381–387. DOI: 10.1071/WF01036

Shin, J.-I.; Seo, W.-W.; Kim, T.; Park, J.; Woo, C.-S. Using UAV Multispectral Images for Classification of Forest Burn Severity—A Case Study of the 2019 Gangneung Forest Fire. Forests 2019, 10, 1025. DOI: 10.3390/f10111025

Stavrakou, T.J., Müller, F., Bauwens, I., De Smedt, C., Lerot, M., Van Roozendael, P.F., Coheur, C., Clerbaux, K.F., Boersma, R., Van der, A., Song, Y. 2016. Substantial Underestimation of Post-Harvest Burning Emissions in the North China Plain Revealed by Multi-Species Space Observations, Scientific Reports 6, Article number: 32307.

Tabi, F.O., Mvondo, A.D., Boukong, A., Mvondo, R.J., Nkoum, G. 2013. Changes in soil properties following slash and burn agriculture in the humid forest zone of Cameroon. African Journal of Agricultural Research 8(18):1990-1995. DOI: 10.5897/AJAR2012.1713

Viana-Soto, A., Aguado, I., Martínez, S. 2017. Assessment of Post-Fire Vegetation Recovery Using Fire Severity and Geographical Data in the Mediterranean Region (Spain). Environments. 4(4):90. DOI: 10.3390/environments4040090

Walker, J., Raison, R.J., Khanna, P.K. 1986. Fire. In Australian Soils. The Human Impact. Russell, J.S., Isbell, R.F., Eds. Queensland University Press: Brisbane. 86:186–216.

Zabala, L.M., De Celis, R., Jordán, A. 2014. How wildfires affect soil properties. A brief review. CIG 40(2):311-321.

Zha, S.P., Zhang, S.Q., Cheng, T.T., Chen, J.M., Huang, G.H., Li, X., Wang, Q.F. 2013. Agricultural Fires and their potential impacts on regional air quality over China. Aerosol and Air Quality Research 13: 992–1001. DOI: 10.4209/aaqr.2012.10.0277

Zhang, X., Kondragunta, S., Schmidt, C., Kogan, F. 2008. Near real time monitoring of biomass burning particulate emissions (PM2.5) across contiguous United States using multiple satellite instruments. Atmospheric Environment 42:6959–6972. DOI: 10.1016/j.atmosenv.2008.04.060